

Performance Analysis of the Force Control for an Electromechanical Feed Axis with Industrial Motion Control

Andre Sewohl¹, Manuel Norberger¹, Chris Schöberlein¹, Holger Schlegel¹ and Matthias Putz^{1,2}

¹*Institute of Machine Tools and Production Processes, Chemnitz University of Technology, Reichenhainer Straße 70, 09126 Chemnitz, Germany*

²*Fraunhofer-Institut for Machine Tools and Forming Technologies, Reichenhainer Straße 70, 09126 Chemnitz, Germany*

Keywords: Electromechanical Feed Axis, Motion Control, Force Control, Controller Design, Controller Performance.

Abstract: Control of process forces provides significant economic benefits for many use cases. The force is often the limiting factor for the design of the processes and the choice of parameters. As a controlled variable, it is predestined to ensure stability and safety of many processes. Direct influence also enables increasing productivity and improving part quality. However, force control has not yet become established for manufacturing processes in machine tools with electromechanical axes and industrial control. A major problem area is the lack of real-time capability. Due to the delay times in signal processing, real-time capability is not guaranteed for dynamic movements of feed axes. High-resolution and fast measurement inputs are particularly relevant here. Industrial control manufacturers have made significant progress in this area. In this publication, the experimental setup of an electromechanical feed axis is presented, which is equipped with new industrial control components. The implementation of the force control is also described. Focus is on the investigations regarding the controller performance. The set point and disturbance behaviour as well as the reaction to the process start are considered.

1 INTRODUCTION

In modern production systems, there is a trend to replace mechanical motion solutions with electrical ones. There are many strategies for controlling machine-specific quantities, such as the position or speed of electromechanical axes. The concept of cascade structure, also called servo control, has become established in this field (Schröder, 2001). The use of controlled electromechanical drive systems can meet the increasing demands on the machines in terms of dynamic behavior, as well as higher productivity and accuracy.

Nevertheless, in the area of production engineering, there are ongoing efforts to improve manufacturing strategies and processes in terms of stability, quality and efficiency. One possibility for ensuring stable process conditions and reducing rejected parts is closed loop control of quality determining parameters (Allwood et al., 2016). The development of suitable control concepts at the process level, in which significant process variables are taken into account as controlled values, offers

considerable scope for improvement at this point. There are many process variables which have an influence to the quality of a part. However, usually it is very difficult to control these values. The metrological acquisition of corresponding parameters constitutes a further challenge.

The machining force is a suitable parameter that can be detected well by measurement. It is of particular relevance for the majority of processes in the field of production technology. As a controlled variable, it is predestined for ensuring process stability and safety. Machining forces are often the limiting factor for the design of the processes and the choice of parameters. Excessive loads can cause damage and defects to the workpiece, tool or machine. In the worst case, they even lead to its destruction. In addition, process forces provide important information about the process state and allow conclusions about deviations in the production process, the machine, the tool, the workpiece or material.

The next chapter provides an overview of the state of the art in force control and research efforts.

In addition, the existing challenges and the need for action are shown. The selected test-setup is presented in the third chapter. Subsequently, performed experiments are explained and consecutively evaluated. The last chapter completes the publication with a summary and description of the conclusions.

2 STATE OF THE ART

Control of process forces provides significant economic benefits for many use cases by increasing operation productivity and improving part quality. Especially for processes in the field of machining technology, targeted influencing of the process forces is of outstanding importance (Ulsoy and Koren, 1993). For this reason, a large number of concepts and algorithms for control of process forces have been investigated and developed both in research and industry.

First significant ideas associated with process control systems were introduced in the 1960's (Ulsoy and Koren, 1989). An early work investigated a PID-structure with fixed gain controller as approach. But it turned out that fixed-gain controllers could not maintain system performance and stability in machining force control (Koren and Masory, 1981). That led to an increasing interest in the development of adaptive machining force controllers. The majority of the work in machining force control is devoted to the subject of adaptive techniques. An overview to the developments in adaptive control systems is given in (Ulsoy et al., 1983). (Liu et al.; 2001) compares different adaptive control techniques. However, adaptive controllers can be difficult to develop, analyze, implement, and maintain due to their inherent complexity. Consequently, adaptive machining force controllers have found little application in industry (Landers et al., 2004).

In recent years, approaches with fuzzy logic controllers have been increasingly investigated (Zuperl et al., 2005), (Xu and Shin, 2008), (Kim and Jeon, 2011). Artificial neural networks also came into focus of considerations increasingly (Haber and Alique, 2004), (Yao et al., 2013). Even a novel approach using predictive algorithms was recently presented in (Stemmler et al., 2017). But these concepts were also unable to establish themselves in industry.

A key problem is that complex control structures and algorithms are difficult to integrate in machine tools with conventional industrial control.

Additional hardware usually has to be used. The resulting communication times in turn reduce performance and reaction speed is limited. Direct access to the control level (e.g. the interpolation cycle) is necessary to ensure real-time capability. In this context, measuring the process forces with additional sensors is also problematic. The cycle time is increased even further through signal processing and integration into the control system. This becomes clear in (Posdlich et al., 2019) for example. The system is superimposed to the control and the entire measuring chain has a sampling time of approximately 40 ms. The control can only react to a limited extent to quickly acting disturbance forces.

High-resolution measurement inputs are particularly relevant for force control, besides real-time capability. The configuration of the load cell with strain gauges is based on maximum loads. As a result, only a small part of the total area remains for the force actually occurring in the process with 12-bit converters. Therefore higher resolutions (16-24 bit) are necessary.

Industrial control manufacturers have made significant progress in these areas. The control components and assemblies from Beckhoff meet these requirements and offer new opportunities. The corresponding experimental test-setup for an electromechanical axis is presented in the next chapter. Here, the implementation options of direct force control are considered and examined with regard to their limits and performance.

With regard to the design of a force control on electromechanical feed axes, no generally applicable regulations are known yet. Accordingly, no auto-tuning functionalities are available on the control side. Since no automatism or reproducible procedure can be applied, the usual practice of manual parameterization is used first. In addition, various setting rules are examined with regard to their suitability.

3 TEST-SETUP

For the experiments, a test-setup of an electromechanical feed axis was selected, which is designed for loads up to 10 kN. The mechanical construction and control engineering structure are described below. The commissioning and enhancement with a force control are elucidated, too.

3.1 Structure of the Drive Train

The basic structure of the test-setup corresponds to a portal construction. However, only one drive is used to generate the movement. The selected standard servomotor AM8031 is suitable for drive solutions with highest demands on dynamics and performance. The rotational movement of the motor is transmitted to a gear via a drivebelt. Another belt-gear connection is used to translate and split the rotation between the two spindles, which are integrated in the frame. The traverse is attached to the two ball screws, which are arranged at the same height. These are used to convert the rotation into a translatory upward and downward movement. Synchronism of the spindles and parallelism of the traverse, which is used for load transfer, are mechanically guaranteed with this construction. The entire drive train with its single transmission elements is illustrated as a CAD-model in Figure 1.



Figure 1: Drivetrain of the electromechanical axis.

3.2 Control Components

A digital compact servo controller of type AX5101 is used appropriate to the servo motor. The system is also equipped with safety modules, analog and digital I/O-modules, an ELM3502 terminal, a power supply terminal and an EtherCAT bus coupler. All components are connected via the backplane bus. Communication with the servo controller and the external PC takes place via the EtherCAT-connection. This structure is illustrated in Figure 2.

The Software TwinCAT 3 (The Windows Control and Automation Technology) automation suite is available on the external PC. It is the core of the control system and can be assigned to PC-based

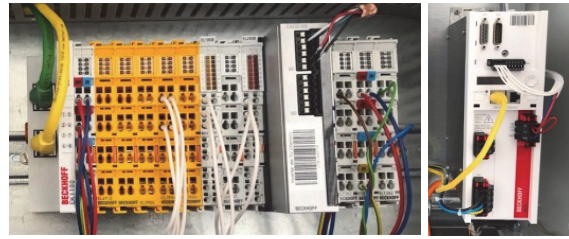


Figure 2: Control engineering of the test-setup.

control technology. The TwinCAT software system from Beckhoff converts almost any PC-based system into a real-time control with several PLC, NC, CNC or RC runtime systems. This software is used, among other things, for programming, configuration and control. The execution system and the execution times can be freely defined and program parts can be assigned to own tasks. The basic architecture of TwinCAT is shown in Figure 3.

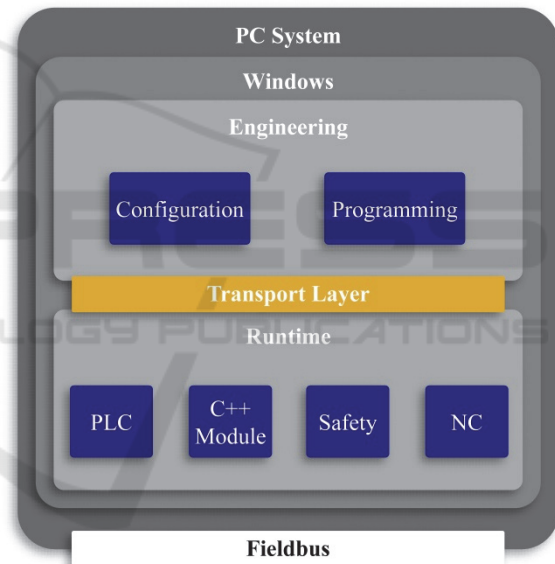


Figure 3: Twin-CAT architecture.

The recently developed ELM3502 terminal is of particular importance in this assembly. It can be used for the measurement bridge evaluation of full, half or quarter bridges. An essential feature is the high resolution of 24 bits with a very fast sampling rate of 50 μ s. This module is used to connect the signals of the force sensor so that direct force control can be implemented on the test-setup. A SSM-AJ-10 kN force sensor from Interface, which is based on strain gauge technology, is used for force measurement.

3.3 Commissioning

During the commissioning of the test-setup, the position control is first implemented to ensure basic functionality. It is designed in a cascade structure. The parameters are set from the inside out, starting with the current control loop. This is based on the performance data and electrical parameters of the motor. The parameters of the current control loop are already defined and set by the manufacturer. Next, the velocity control loop is superimposed. Autotuning algorithms for drive control are currently still being developed at Beckhoff. Therefore, the velocity controller is commissioned using the Ziegler-Nichols method, which is frequently used in practice. For this purpose, the gain factor of the speed controller was increased up to the stability limit. Then the gain to be set corresponds to 45 % of the critical value. The reset time for the PI controller corresponds to 85 % of the oscillation frequency. The gain factor K_v of the position controller is calculated according to the specification of (Zirn, 2008). This depends on the damping of the system. With a damping value of 1, the system is not vibratory. The following equation applies here:

$$K_v = 1 / (4 * T_{eq,n}) \tag{1}$$

The equivalent time constant of the speed control loop can be determined from the frequency response using the following equation:

$$T_{eq,n} = 1 / (2\pi * \omega_b) \tag{2}$$

The parameter ω_b corresponds to the bandwidth that is at the intersection of the amplitude response with the -3dB line. The corresponding frequency response is shown in Figure 4.

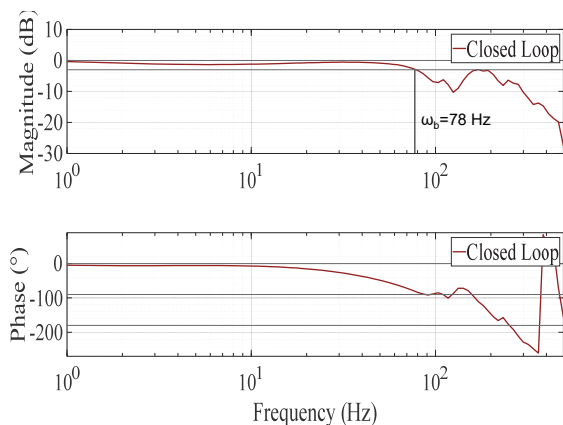


Figure 4: Frequency response of the velocity control loop.

The bandwidth is 78 Hz, which results in an equivalent time constant of 2 ms. The gain factor K_v is thus 125 s^{-1} . The parameters of the cascade control are summarized in Table 1.

Table 1: Controller parameter.

Current controller	Gain factor	$K_{P,i} = 402 \text{ [V/A]}$
	Reset time	$T_{n,i} = 0,8 \text{ [ms]}$
Velocity controller	Critical gain factor	$K_{crit} = 0,14 \text{ [Nms/rad]}$
	Period of oscillation	$T_{crit} = 11 \text{ [ms]}$
	Gain factor	$K_{P,v} = 0,063 \text{ [Nms/rad]}$
	Reset time	$T_{n,v} = 9,3 \text{ [ms]}$
Position controller	Gain factor	$K_v = 125 \text{ [s}^{-1}\text{]}$

4 FORCE CONTROL

4.1 Control Structure

The position control is essential for movements in order to comply with defined position specifications. The force control shall be used at the start of the process to influence the process forces. Accordingly, it is necessary to enhance the existing cascade control with the force control. Here it makes sense to implement the combination of the two controllers by switching. The switchover can take place on the basis of specified boundary conditions and is based on the application scenarios. Here, for example, reaching a predetermined position is an option. However, a force threshold is more suitable for detecting the start of the process. When a force is detected, the control is switched over so that a target force can be specified. Therefore, a force limit value is first defined as a switchover condition on the test-setup.

There are several options for integrating the force controller into the structure. At this point it is crucial that the cycle times of the individual controllers in the cascaded position control are different. The cycle time of the current controller is shorter than that of the speed controller, which in turn is shorter than that of the position controller. An overlay on the position control loop would mean a further slowdown. In order to be able to react quickly and to be robust at the same time, it is advisable to implement the force controller on the same level as the position controller. As a result, both controllers have the same manipulated variable and the velocity controller also receives its set point from the force controller. In this case, the control

difference is transferred to the velocity controller as a speed set point via the force controller. This offers another advantage. In order to be able to specify the speed set point, either a corresponding variable can be applied in the control loop or the IEC 61131-3-compliant motion control (MC) commands are used. The MC blocks are available in a library and are instantiated in the programs. The parameters are set in the state machine. The MC_MoveVelocity was utilized in detail, which gives a speed set point via the NC axis technology object to the servo inverter and thus the velocity controller. This results in the structure for force control as illustrated in Figure 5.

4.2 Experiments and Parameterization

With regard to the design of a force control on electromechanical feed axes, no generally applicable regulations are known yet. For this reason, manual parameterization is carried out first. When controlling process forces, the process itself is part of the controlled system. Accordingly, the control plant of the force controller consists of the subordinate velocity and current control loop, as well as the mechanics of the axis and the process. In order to simulate a process or a resulting process force, a flexible spring element with a linear characteristic was selected. In this way, a load with high reproducibility can be initiated with a movement of the axis against the resistance. A P-controller was initially selected as the controller type. This is justified by the fact that P-controllers can be designed quickly and easily with just one parameter. Moreover, the fact that the controlled system or the process already contains an integrating part can be exploited. Furthermore, it makes sense to

integrate an actual value filter in the control loop in order to reduce the measurement noise and improve the signal quality. A moving average filter with a time window of 10 ms was selected for this purpose.

In addition, it should be investigated to what extent general setting regulations from the time range can be used for the design of the force control. Hence, it is necessary to carry out an identification of the control plant, which includes the process or the flexible spring, respectively. During identification, a stepwise excitation of 5 mm/s is activated at the input of the velocity control loop. A speed offset of 1 mm/s was determined in order to avoid static friction effects. The force is recorded at the output of the control plant. The result of the identification and the relevant parameters are shown in Figure 6 and summarized in Table 2.

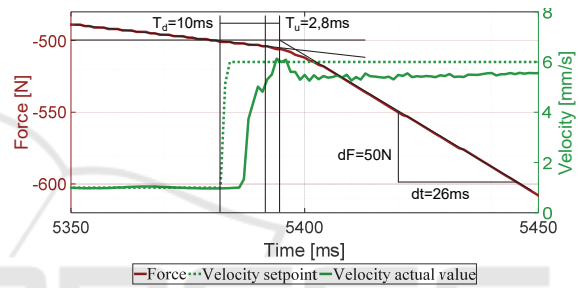


Figure 6: Identification of the controlled system.

Table 2: Controlled system parameters.

Time difference	$dt = 26 \text{ ms}$
Force difference	$dF = 50 \text{ N}$
Actual velocity	$v_{av} = 5,5 \text{ mm/s}$
Dead time	$T_d = 10 \text{ ms}$
Delaying time	$T_u = 2,8 \text{ ms}$

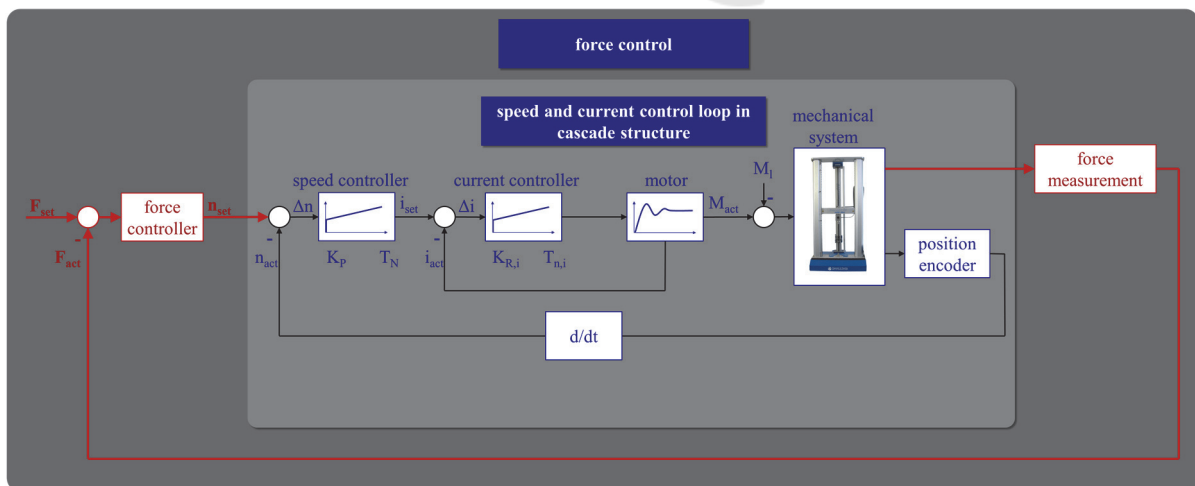


Figure 5: Force control structure.

The controlled system has an IT1 behavior and the gain can be calculated according to the following equation:

$$K_{SI} = dF / (dt * v_{av}) \tag{3}$$

Based on the determined values, K_{SI} is 350 N/mm. The gain factor for the force controller can be calculated on the basis of these characteristic values. For this purpose, Samal's setting instruction (Lunze, 2005):

$$K_P = \pi / (4 * K_{SI} * (T_d + T_u)) \tag{4}$$

and the calculation of the symmetrical optimum according to (Lutz and Wendt, 1995):

$$K_P = 1 / (a * K_{SI} * (T_d + T_u)) \tag{5}$$

were selected. Here, the parameter a is a damping factor that has been set to the value 2. The calculated parameters are summarized in Table 2.

Table 2: Parameters for the force control.

adjustment rule	Parameter
Samal	$K_P = 175 * 10^{-3}$ [mm/Ns]
Symmetrical Optimum	$K_P = 112 * 10^{-3}$ [mm/Ns]

To assess the controller behavior, a preload of 500 N was first generated and subsequently a force jump of 50 N was specified for the closed control loop. The step responses for the different amplification factors with the unit [10⁻³ mm/Ns] are shown in Figure 7.

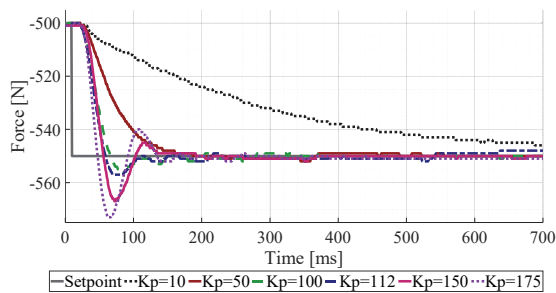


Figure 7: Step response of the controllers.

The controller performance is assessed on the basis of comparison criteria in the time domain. The rise and set time as well as the overshoot were selected as criteria. A tolerance band of ± 2 N was defined for this. The characteristic values for the different parameterizations are compared in Table 3.

Table 3: Comparison criteria in the time domain.

K_P [10 ⁻³ m/Ns]	Rise time [ms]	Set time [ms]	Overshoot [N]
10	721	721	-
50	177	177	-
100	57	132	5
112	49	89	7
150	46	120	17
175	37	121	23

In Figure 7 it can already be clearly seen that the rise time becomes smaller with increasing amplification factor. However, the overshoot range is also increasing. With sufficiently small amplification factor, no overshoot occurs. Moreover, dead time of 15 ms was identified for the system. Finally the adjustment rule based on the symmetrical optimum offers a good compromise between overshoot height and rise time.

Another interesting aspect to investigate is the system behavior in the case of contact. The start of the process should be recognized automatically based on the threshold force of 1,5 N and trigger the switch from position control to force control. A constant velocity was specified in order to cause a contact situation and to simulate an disturbing process force. The setpoint of the force is 0 N, so that the disturbance caused by the contact is corrected. For this, the parameterization according to the symmetrical optimum was first selected and the behavior at different velocities was considered. The gain factor was then varied at a velocity of 5 mm/s. The results are illustrated in Figure 8.

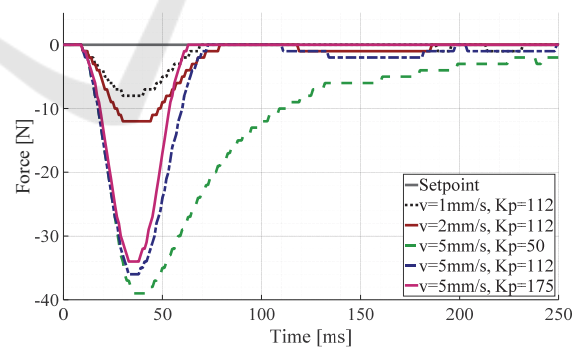


Figure 8: System behavior in case of contact.

Due to the dead time during the switchover, the starting velocity has the greatest influence on the height of the acting force. The amplification factor has an influence, too. The greater the amplification factor is chosen, the smaller is the force. However, this influence is marginal compared to the impact of the starting velocity. On the other hand, the gain factor has major impact on the settling time. The

higher the factor is selected, the faster the disturbance can be corrected. At some point a saturation effect occurs here. There is only a slight difference between adjustment instruction accordingly Samal and the symmetrical optimum. A further increase in the gain would therefore only have a minor effect.

By switching from the position control, it is possible to specify a force profile. It is important to examine how well the controller follows the set point. For the experiment, a positioning ramp is initially specified, which is replaced by a set point force curve at a threshold of 500 N. A force increase of 100 N/s up to a force of 1000 N was specified here. The system behavior of different parameter settings is shown in Figure 9.

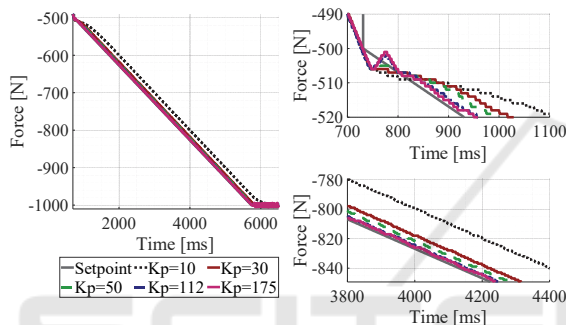


Figure 9: System behavior for a defined force curve.

Due to the dead time when switching, the starting velocity is initially maintained. The force control reacts after the dead time of 15 ms. With bigger gain factors, there is then a slight overshoot (see Figure 9, up right). However, the contouring error is significantly smaller here (see Figure 9, down right). These values are summarized in Table 4.

Table 4: Comparison Criteria of the force ramp.

K_p	Overshoot	Contouring error	Delay time
10	-	27 N	270 ms
30	-	10 N	84 ms
50	-	5 N	51 ms
112	3 N	2 N	21 ms
175	4 N	2 N	15 ms

Here, the difference between the adjustment instruction accordingly Samal and the symmetrical optimum is also only marginal. Overall, the adjustment rule of the symmetrical optimum is a suitable criterion for the parameterization of the force controller for this use case.

Moreover, the effect of the actual value filter setting on the control was also examined. Different filter time windows for the gain factor of the symmetrical optimum were compared. Here, the force curve was specified again. The results are shown and summarized in Figure 10.

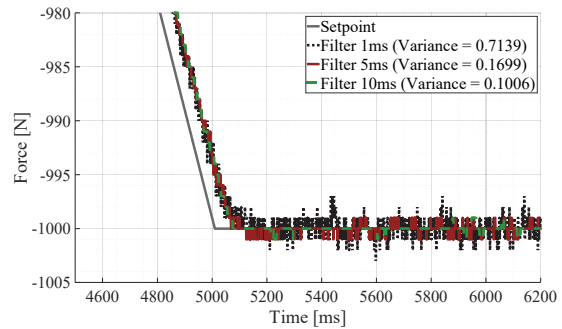


Figure 10: Influence of the force actual value filter.

It can be seen that a significant reduction in measurement noise can be achieved with the length of the sliding window. The variance of the measured value decreases with increasing length and satisfactory results are achieved at 10 ms.

5 CONCLUSION

In this publication, the combination of force control with position control was presented for an electromechanical axis. The focus of the investigations was on the controller performance. Empirical setting factors and general adjustment rules were evaluated with regard to their suitability. It has been found here that good results can be achieved with the symmetrical optimum. It was also shown that the functionality of the switchover is given. Moreover, the force is quickly adjusted in the case of contact. In addition, the control follows specified force profiles with a small contouring error. If necessary, this can be reduced even further with a feedforward control.

The external PC was initially used for commissioning and implementation. The performance was assessed for this system structure. A system expansion with a top-hat rail industrial PC is perspective possible and also envisaged. It can be integrated directly via the backplane bus. This requires porting the project to the IPC. In this way, the communication dead times due to the EtherCAT connection are eliminated and a further improvement in performance can be expected. The implementation of the corresponding measures is

planned in future studies. The potential of complex control algorithms should also be considered there.

ACKNOWLEDGEMENTS



European Union



Funded by the European Union (European Social Fund) and the Free State of Saxony.

REFERENCES

- Schröder, D., 2001. *Elektrische Antriebe – Regelung von Antriebssystemen*, Springer Verlag Berlin, 2nd edition.
- Allwood, J. M., et al., 2016. Closed-loop control of product properties in metal forming. In *CIRP Annals – Manufacturing Technology*, 65, 573-596.
- Ulsoy, A.G. and Koren, Y., 1993. Control of Machining Process. In *Journal of Dynamic Systems Measurement and Control*, 115, 301-308.
- Ulsoy, A.G. and Koren, Y., 1989. Applications of adaptive control to machine tool process control. In *IEEE Control Systems Magazine*, 9(4), 33-37.
- Koren, Y. and Masory, O., 1981, Adaptive Control with Process Estimation. In *CIRP Annals*, 30(1), 373-376.
- Ulsoy, A.G., Koren, Y. and Rasmussen, F., 1983. Principal developments in the adaptive control of machine tools. In *Journal of Dynamic Systems, Measurement, and Control*, 105(2), 107-112.
- Liu, Y., Cheng, T. and Zuo, L., 2001. Adaptive control constraint of machining processes. In *The International Journal of Advanced Manufacturing Technology*, 17(10), 720-726.
- Landers, R.G., Ulsoy, A.G. and Ma, Y.-H., 2004. A comparison of model based machining force control approaches. In *International Journal of Machine Tools and Manufacture*, 44(7-8), 733-748.
- Zuperl, U., Cus, F. and Milfelner, M., 2005, Fuzzy Control Strategy for an Adaptive Force Control in End-Milling, In *Journal of Materials Technology*, 164-165, 1472-1478.
- Xu C. and Shin Y.C., 2008. An adaptive fuzzy controller for constant cutting force in end-milling processes. In *Journal of Manufacturing Science and Engineering*, 130 (3).
- Kim, D. and Jeon, D., 2011. Fuzzy-logic control of cutting forces in CNC milling processes using motor currents as indirect force sensors. In *Precision Eng.*, 35(1), 143-152.
- Haber, R.E. and Alique, J.R., 2004. Nonlinear internal model control using neural networks: an application for machining processes. In *Neural Computing & Applications*, 13, 47-55.
- Yao, X., et al., 2013. Machining force control with intelligent compensation. In *International Journal of Advanced Manufacturing Technology*, 69, 1701-1715.
- Stemmler, S., et al., 2017. Model Predictive Control for Force Control in Milling. In *IFAC-PapersOnLine*, 50(1), 15871-15876.
- Posdziej, M., et al., 2019. Burnishing of prismatic workpieces on three-axis machine enabled by closed loop force control. In *52nd CIRP Conference on Manufacturing Systems (CMS)*, 81, 1028-1033.
- Zirn, O., 2008. Machine Tool Analysis – Modelling, Simulation and Control of Machine Tool Manipulators. Habilitation, ETH Zürich.
- Lunze, J., 2005. *Regelungstechnik 1: Systemtheoretische Grundlagen, Analyse und Entwurf einschleifiger Regelungen*, Springer Vieweg, Heidelberg, 5th edition.
- Lutz, H. and Wendt, W., 1995. *Taschenbuch der Regelungstechnik*, Harri Deutsch, Frankfurt, 1st edition.